

# Dye Stabilization and Enhanced Photoelectrode Wettability in Water-Based Dye-Sensitized Solar Cells through Post-assembly Atomic Layer Deposition of TiO<sub>2</sub>

Ho-Jin Son,<sup>†</sup> Chaiya Prasittichai,<sup>†,‡</sup> Joseph E. Mondloch,<sup>†</sup> Langli Luo,<sup>‡</sup> Jinsong Wu,<sup>‡</sup> Dong Wook Kim,<sup>†</sup> Omar K. Farha,<sup>\*,†</sup> and Joseph T. Hupp<sup>\*,†,§</sup>

<sup>†</sup>Department of Chemistry and Argonne-Northwestern Solar Energy Research (ANSER) Center, Northwestern University, Evanston, Illinois 60208, United States

<sup>‡</sup>Department of Materials Science and Engineering, NUANCE Center, Northwestern University, Evanston, Illinois 60208, United States

<sup>§</sup>Argonne National Laboratory, 9700 South Cass Avenue, Argonne, Illinois 60439, United States

## Supporting Information

**ABSTRACT:** Detachment (desorption) of molecular dyes from photoelectrodes is one of the major limitations for the long-term operation of dye-sensitized solar cells. Here we demonstrate a method to greatly inhibit this loss by growing a transparent metal oxide (TiO<sub>2</sub>) on the dye-coated photoelectrode via atomic layer deposition (ALD). TiO<sub>2</sub>-enshrouded sensitizers largely resist detachment, even in pH 10.7 ethanol, a standard solution for intentional removal of molecular dyes from photoelectrodes. Additionally, the ALD post-treatment renders the otherwise hydrophobic dye-coated surface hydrophilic, thereby enhancing photoelectrode pore-filling with aqueous solution.

Dye-sensitized solar cells (DSCs), the best of which can now achieve light-to-electrical energy conversion efficiencies ( $\eta$ ) of >12%, are widely considered to be among the most promising alternatives to conventional silicon-based solar cells.<sup>1</sup> DSCs employ an electrolyte solution (redox-active salt + organic solvent) and rely upon the formation of a high-area solution/semiconductor interface. One practical limitation of existing DSC designs is the tendency, over time, for dyes to detach (desorb) from the photoelectrode.<sup>2,3</sup> Once detached, these sensitizers no longer contribute photocurrent, thereby resulting in lower cell performance. This behavior is thought to be due to competitive adsorption of water, which may enter the cell over time via capture of moisture from air. (A typical rate is 0.01 g/m<sup>2</sup> day.)<sup>4,5</sup> A second practical problem is a degradation of cell performance when the conventional redox-electrolyte-containing organic solvent is replaced by water as solvent.<sup>6</sup> The performance shortfall is thought primarily to reflect problems in getting aqueous solutions to completely permeate high area photoelectrodes. Nevertheless, the ability to use water as the solvent would reduce materials costs and make cells greener by eliminating hazards associated with disposal or leakage. Thus, the development of methods for preventing desorption and for facilitating aqueous electrolyte use would clearly be desirable.

Recent DSC work that could potentially be relevant to stabilizing dyes against desorption, includes (a) polymerization

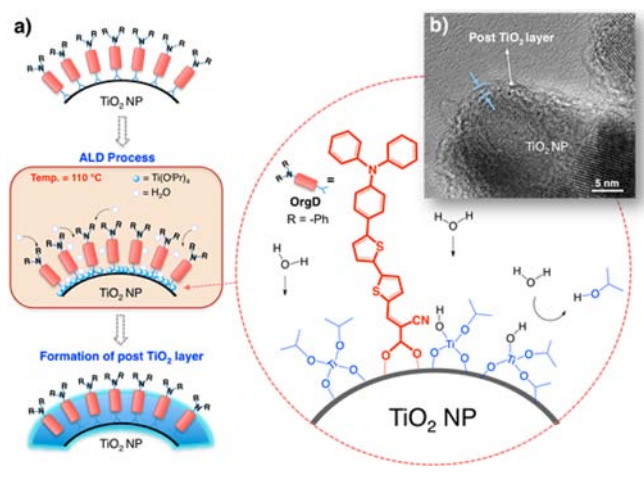
(cross-linking) of molecules co-adsorbed with dyes<sup>7</sup> and (b) glass encapsulation of dyes following photoelectrode adsorption.<sup>8</sup> The second approach, while attractive for other reasons, struck us as potentially problematic for use with aqueous DSCs (especially under basic conditions) because of the finite solubility of silica in water. Nevertheless, because glass encapsulation of dyes was accomplished by using an approach closely related to ALD, we reasoned that direct ALD of a metal-oxide material might be a viable way of protecting molecular anchoring groups against displacement from an electrode surface. Such a protective layer could function by physically blocking water molecules or hydroxide ions from reaching the anchoring site, and/or by enabling an anchoring oxygen atom (from a carboxylate) to interact with multiple metal cations. ALD additionally seemed well suited due to its remarkably conformal coating behavior,<sup>9</sup> its comparatively low deposition-temperature requirements (typically <150 °C),<sup>10</sup> and its high resolution with regard to thicknesses of deposited layers.<sup>11,12</sup> While our focus below is on neutral and basic solutions, the envisaged strategy was further supported by our recent finding that carboxylate-anchored dyes in multi-chromophore DSCs can be protected against acid-induced (aqueous HF) desorption by first treating dye/TiO<sub>2</sub> photoelectrode assemblies with several ALD cycles of metal oxide.<sup>13</sup>

Herein, we present the results of post-assembly ALD of ultrathin coatings of TiO<sub>2</sub> on **OrgD**-sensitized, nanoparticulate TiO<sub>2</sub> electrodes.<sup>14</sup> (See Scheme 1; **OrgDH** = (*E*)-2-cyano-3-(*S'*-(*S''*-(*p*-(diphenylamino)phenyl)thiophen-2''-yl)thiophen-2'-yl)-acrylic acid.) TiO<sub>2</sub> was selected as the coating material due to its extraordinary chemical stability, even under extremes of pH;<sup>15</sup> its known shielding/scavenging activity toward humidity and O<sub>2</sub>;<sup>16–19</sup> and its compositional matching with the underlying electrode. Water and titanium(IV) tetraisopropoxide were used to grow TiO<sub>2</sub> in controlled fashion. ALD was performed at 110 °C so as to avoid thermal degradation of the dye. (We have previously shown that under anaerobic conditions **OrgD** can withstand reactor temperature excursions to at least 170 °C.<sup>8</sup>)

Received: June 27, 2013

Published: July 22, 2013

**Scheme 1.** (a) Schematic Depiction of Post-assembly Atomic Layer Deposition of  $\text{TiO}_2$  and (b) HR-TEM Image of Post-treated  $\text{TiO}_2\text{:OrgD}/10 \text{ TiO}_2$  ALD Film



With an eye toward generalizing the approach, however, we sought to employ much lower temperatures. Details regarding the deposition protocol can be found in the Supporting Information (SI). Under the conditions of our experiments, the growth rate of  $\text{TiO}_2$  as determined by ellipsometry on flat silicon platforms, was found to be  $\sim 1 \text{ \AA}$  per ALD cycle (Figure S1). High-resolution TEM measurements (Figure S9) established that the growth rate is unchanged for dye-covered nanoparticulate  $\text{TiO}_2$  and that the coating is uniform and conformal. Quartz crystal microbalance (QCM) measurements corroborated that ALD occurs on **OrgD**-coated NP electrodes and established that the rate of growth is uniform. (See Figure 1 (inset) and Figure S2.)

The intensity of the broad visible-region absorption spectrum of **OrgD** on nanoparticulate  $\text{TiO}_2$  films is not significantly altered by subsequent ALD of additional  $\text{TiO}_2$  (Figure S3)—implying that the dye is not degraded by metal-oxide formation.<sup>20</sup> As shown in Figure 1, however, the **OrgD** absorbance wavelength maximum,  $\lambda_{\text{max}}$  is affected. The peak shifts red by about 2 nm per

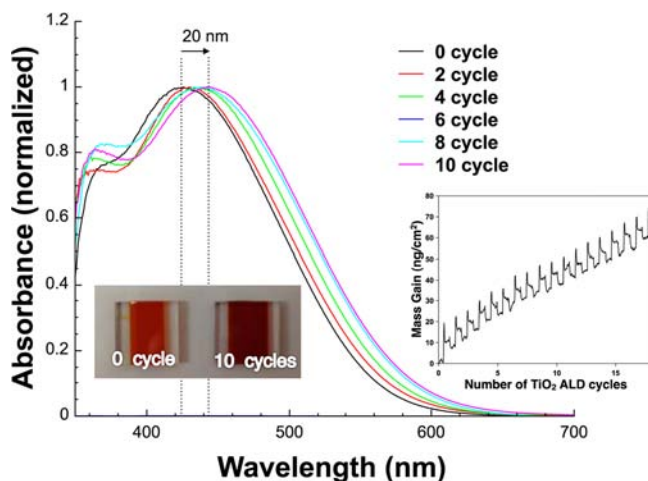


**Figure 1.** Comparison of UV-vis spectra of untreated and post-assembly-coated **OrgD**: $\text{TiO}_2$  nanoparticle film electrodes and photo-images of control (0 cycle) and post-treated film (10 cycles of post  $\text{TiO}_2$  ALD) (inset, below left). QCM mass gain profiles acquired over 18 cycles of QCM(Au)/ $\text{TiO}_2$  ALD/**OrgD** (inset, below right).

ALD cycle for the first ten cycles, with little additional shift occurring thereafter. In view of the donor–acceptor character of **OrgD**, significant shifts in  $\lambda_{\text{max}}$  can be expected whenever the polarity or dielectric strength of the local environment is altered.<sup>21</sup> Indeed, in solution environments the dye is solvatochromic (and pH dependent). In the present study the initial environment (vacuum + neighboring dyes) is changed to  $\text{TiO}_2$ , a high-dielectric semiconductor. The spectral results suggest that **OrgD** is largely encapsulated when the thickness of the ALD coating reaches 10  $\text{\AA}$ . (Notably, no spectral shift is observed upon ALD-encapsulation with  $\text{Al}_2\text{O}_3$ , a low dielectric material.) Additional experiments (cyclic voltammetry; Figure S6) show that **OrgD** remains electrochemically addressable after ALD.

With modified structures in hand ( $\text{TiO}_2\text{:OrgD}/8 \text{ TiO}_2$  ALD) we examined their ability to resist dye loss to solution. Although water is the nominal culprit, the competitive adsorbate almost certainly instead is hydroxide ion. Commonly included at high concentration ( $\sim 0.5 \text{ M}$ ) in nonaqueous electrolyte solutions for DSCs, because of its propensity to suppress dark currents, is *tert*-butylpyridine (TBP). As a reasonably effective Brønsted base, TBP can be expected to extract protons and convert any residual or moisture-derived water molecules in DSC solutions nearly quantitatively to hydroxide ions. We reasoned, therefore, that accelerated tests of dye desorption could be done by employing a receiver solution of ethanol (desirable because of the typically high solubility of organic dyes in this solvent) that had intentionally been made basic by addition of NaOH. Ideally, the acceleration protocol would cause unprotected dye molecules to be desorbed in minutes or hours rather than months or years. As detailed below, ethanolic solutions with apparent pH of 10.7 proved suitable (i.e., 0.5 mM NaOH).

Shown in Figure 2a,b are visible-region absorption spectra for  $\text{TiO}_2\text{:OrgD}/8 \text{ TiO}_2$  ALD and  $\text{TiO}_2\text{:OrgD}$ , respectively,

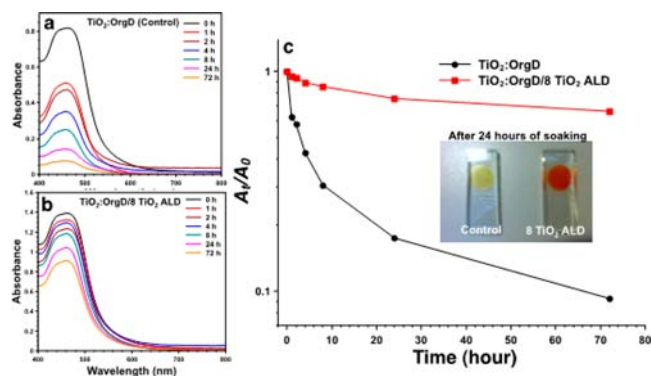


**Figure 2.** Left: visible-region spectra of  $\text{TiO}_2\text{:OrgD}$  (control) after exposure for 0–72 h (a) and  $\text{TiO}_2\text{:OrgD}/8 \text{ TiO}_2$  ALD (b). The thickness of each film was  $3 \mu\text{m}$ . Right: relative  $A_t/A_0$  absorbance of  $\text{TiO}_2\text{:OrgD}$  (black) and  $\text{TiO}_2\text{:OrgD}/8 \text{ TiO}_2$  ALD (red) at 460 nm after soaking in ethanol containing 0.5 mM NaOH and photos of films after soaking both types for 24 h.

following soaking basic for times ranging from 0 to 72 h. Figure 2c shows the absorbance at various times  $t$  relative to the initial absorbance (i.e.,  $A_t/A_0$ ). To facilitate comparisons, the relative absorbance is presented on a  $\log_{10}$  scale. Even on this scale, the unprotected dye can be seen to desorb much more rapidly than the ALD-protected version. As the photograph in the inset to panel c shows, after 24 h the initially intense orange  $\text{TiO}_2\text{:OrgD}$  electrode has become pale yellow, while  $\text{TiO}_2\text{:OrgD}/8 \text{ TiO}_2$

ALD assembly remains strongly colored. A comparison of approximate half-lives for dye loss shows that treatment of an electrode with eight ALD cycles ( $\text{TiO}_2$ ) slows desorption process by about 1.5 orders of magnitude, i.e., roughly 50-fold. Nevertheless, after three days in basic EtOH, significant desorption of even the ALD-protected dye is evident. It would be interesting to see if desorption rates are similarly slowed for dyes that are much more strongly and persistently adsorbed, for example, dyes that utilize phosphonate,<sup>14,22–25</sup> acetyl acetate,<sup>26–28</sup> or hydroxamate<sup>29</sup> as anchors.

As shown further by data in the SI, the stabilizing effect of ALD  $\text{TiO}_2$  extends to the ruthenium-based dyes, N719 and Z907, in water as the solvent—albeit, to a lesser degree than observed with **OrgD** in basic EtOH (see Figures S15, S16, and S18).

It is notable that the surface energy of  $\text{TiO}_2$ :**OrgD** photoelectrodes, as gauged by water contact-angles ( $\theta_{\text{water}}$ ), is significantly changed by post-assembly ALD of  $\text{TiO}_2$ . As shown in the photos in Figure 3, prior to ALD the surface is

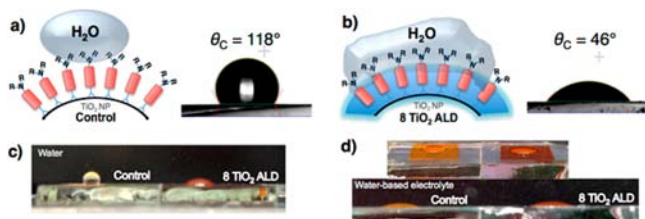


**Figure 3.** Photos and idealized cartoons (limiting cases) of water droplet shape on (a)  $\text{TiO}_2$ :**OrgD** film with a contact angle of  $118 \pm 0.9^\circ$  and (b)  $\text{TiO}_2$ :**OrgD**/8  $\text{TiO}_2$  ALD film with a contact angle of  $46 \pm 1.5^\circ$ . Photos of (c) water and (d) water-based electrolyte used in actual DSC droplet shape on ALD-free and ALD-post-treated electrode films.

hydrophobic, but after ALD it is hydrophilic. The initial hydrophobicity is to be expected, given the phenyl terminating groups of adsorbed **OrgD**. As suggested by the cartoons in Figure 3a,b, and supported by the observations above regarding asymptotic **OrgD** spectral shifts with increasing numbers of ALD cycles, we interpret the hydrophilic behavior of the modified electrode as arising from extension of  $\text{TiO}_2$  to near the dye termini via ALD-based filling of dye-layer interstices. Thus, the aqueous solution is able to contact the metal-oxide without first penetrating the dye layer. Based on the model and experimental observations of O'Regan and co-workers,<sup>6</sup> (a) local hydrophilicity should engender solution permeation of photoelectrode mesopores but (b) local hydrophobicity should constrain dye/aqueous solution and electrode/aqueous solution contact, and limit photocurrent output.

With these differences in mind, we compared the performance of DSCs containing either ALD-treated or ALD-free photoanodes in aqueous electrolyte solution (0.05 M  $\text{I}_2$ , 2 M 1-butyl-3-methylimidazolium iodide (BMII), 0.1 M guanidinium thiocyanate (GuSCN), and 0.5 M TBP). (The higher-than-typical concentration of BMII was used to ensure dissolution of other components in water.<sup>6</sup>) For simplicity, we examined comparatively thin photoelectrodes (6  $\mu\text{m}$ , rather than the 10–12  $\mu\text{m}$  thickness typically used when seeking maximum DSC efficiencies). Additionally, we omitted the  $\text{TiO}_2$  light-scattering layer (large-particle layer) typically used to enhance red-edge photocurrent, since our goal here is not to produce a champion DSC, but to understand what limits DSC performance. In the aqueous DSCs, the untreated  $\text{TiO}_2$ :**OrgD** electrodes gave a short-circuit photocurrent density ( $J_{\text{sc}}$ ) of 3.66  $\text{mA}/\text{cm}^2$ , an

open-circuit photovoltage ( $V_{\text{oc}}$ ) of 640 mV, an overall cell fill-factor (FF) of 0.61, and  $\eta = 1.44\%$ . Under the same conditions, the post-assembly ALD-treated photoelectrodes (8 cycles) yielded significantly better performance:  $J_{\text{sc}} = 4.41 \text{ mA}/\text{cm}^2$ ,  $V_{\text{oc}} = 660 \text{ mV}$ , FF = 0.70, and  $\eta = 2.05\%$  (Table 1). (Similar results were obtained with 10 and 12 ALD cycles.)

**Table 1. Photovoltaic Performance of DSCs**

sample	$J_{\text{sc}}$ [ $\text{mA}/\text{cm}^2$ ]	$V_{\text{oc}}$ [V]	FF	$\eta$ [%]
control (water)	3.66	0.64	0.61	1.44
post-treated (water)	4.41	0.66	0.70	2.05
control ( $\text{CH}_3\text{CN}$ )	2.55	0.58	0.53	0.79
post-treated ( $\text{CH}_3\text{CN}$ )	3.75	0.57	0.72	1.56

At first glance, the findings seem to mirror those of O'Regan<sup>6</sup>—implying that the increased  $J_{\text{sc}}$  in ALD-treated cells can be understood in terms of enhanced access of the aqueous electrolyte to the highly porous, but initially hydrophobic, photoelectrode surface. However, in contrast to the findings of Law et al. who examined a more hydrophobic dye,<sup>6</sup> further studies of **OrgD** ( $J_{\text{sc}}$  vs light intensity, Figure S12) showed that transport limitations on  $J_{\text{sc}}$  are negligible at 1 sun and become significant only at ca. 1.25 and 1.75 sun (for ALD-free and ALD-treated electrodes). Additional measurements of  $\theta_{\text{water}}$  showed that *both* types of electrodes are wetted by water once BMII (a known surfactant) is included in cell solutions. Finally, measurements in  $\text{CH}_3\text{CN}$  as solvent (Table 1) show similar enhancements of  $J_{\text{sc}}$  and  $\eta$  following ALD treatment, thereby ruling out hydrophobic/hydrophilic effects as the cause of the enhancements.

In an effort to understand how ALD post-treatment enhances cell efficiency, we examined back electron-transfer (ET) reactivity. To our surprise, back ET, and therefore the efficiency of current collection, is unaffected by ALD treatment. Ultimately we traced the efficiency effects to increases in the efficiency for electron injection. We intend to report in detail on this behavior elsewhere. Briefly, however, ALD post-treatment serves to break up poorly electron-injecting aggregates of **OrgD**.

Returning to stability studies, the consequences of accelerated thermal aging (60  $^\circ\text{C}$ , aqueous electrolyte, dark with periodic illumination to measure  $\eta$ ) were examined. After 150 h,  $\eta$  values of untreated DSCs dropped by ca. 50% (mainly due to lower  $J_{\text{sc}}$ ; Figure 4a). The decreases are ascribed to dye desorption. In contrast,  $\eta$  and  $J_{\text{sc}}$  values for the ALD-treated cell are little affected, even after 200 h (Figure 4).

In summary, functional encapsulation of carboxylate-anchored molecular sensitizers on high-area  $\text{TiO}_2$  photoelectrodes is achievable via post-assembly ALD of additional  $\text{TiO}_2$ . The ALD

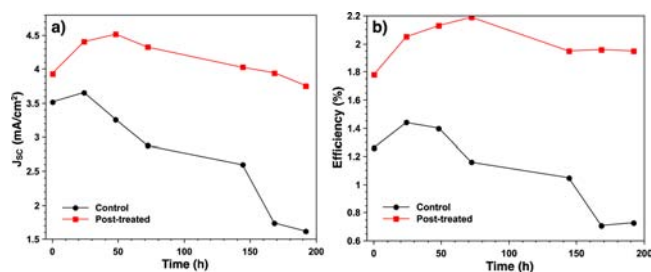


**Figure 4.** Time evolution of  $J_{\text{sc}}$  (a) and  $\eta$  (b) for  $\text{TiO}_2$ :**OrgD** (black) and  $\text{TiO}_2$ :**OrgD**/8  $\text{TiO}_2$  ALD (red) DSCs in aqueous electrolyte. These cells were aged at 60  $^\circ\text{C}$  in the dark.

treatment serves to isolate and protect dye-anchoring groups from displacement by water molecules or hydroxide ions. As a consequence, under conditions designed to achieve rapid dye desorption (i.e., accelerated stability testing) the rate of desorption is slowed by ca. 50-fold. Similarly, accelerated thermal aging studies of water-based DSCs show that post-assembly ALD may be a solution to the broader problem of long-term DSC instability.

The ALD treatment additionally serves to make the initially hydrophobic surface of a representative organic-dye/TiO<sub>2</sub>-photoelectrode assembly significantly hydrophilic. Such change, in turn, suggests that the post-assembly TiO<sub>2</sub> ALD treatment could facilitate permeation of the assembly's mesopores by aqueous electrolyte, boost the fraction of adsorbed dyes that are redox accessible, and enhance the ability of the DSC to function with water as solvent. Stabilization of DSCs via ALD of other metal-oxides as well as application to different types of dyes is currently being investigated.

## ■ ASSOCIATED CONTENT

### ■ Supporting Information

Description of experimental conditions and results of ellipsometry, QCM, voltammetry, UV-vis absorption, HR-TEM, DSC  $J$ - $V$ , and  $V_{oc}$  decay measurements. This material is available free of charge via the Internet at <http://pubs.acs.org>.

## ■ AUTHOR INFORMATION

### Corresponding Author

[o-farha@northwestern.edu](mailto:o-farha@northwestern.edu); [j-hupp@northwestern.edu](mailto:j-hupp@northwestern.edu)

### Present Address

<sup>†</sup>C.P.: Department of Chemical Engineering, Stanford University

### Notes

The authors declare no competing financial interest.

## ■ ACKNOWLEDGMENTS

This work was supported as part of the ANSER Center, an Energy Frontier Research Center funded by the U.S. Department of Energy, Office of Science, Office of Basic Energy Sciences under Award DE-SC0001059. We acknowledge the Thailand's Commission on Higher Education for providing partial graduate support for CP through its program on Strategic Fellowships for Frontier Research Networks. This research was supported in part by the DOE EERE Postdoctoral Research Awards, EERE Fuel Cell Technologies Program, administered by ORISE for DOE. ORISE is managed by ORAU under DOE contract DE-AC05-06OR23100 (J.E.M.). The electron microscopy work was performed in the electron instrumentation center (EPIC) facility of NUANCE center (supported by NSF-NSEC, NSF-MRSEC, Keck Foundation, and the state of Illinois) at Northwestern University.

## ■ REFERENCES

- (1) Yella, A.; Lee, H.-W.; Tsao, H. N.; Yi, C.; Chandiran, A. K.; Nazeeruddin, M. K.; Diau, E. W.-G.; Yeh, C.-Y.; Zakeeruddin, S. M.; Grätzel, M. *Science* **2011**, *334*, 629–634.
- (2) Desilvestro, H.; Bertoz, M.; Tulloch, S.; Tulloch, G. *Dye-Sensitized Solar Cells*, 1st ed.; EPFL Press: Lausanne, Switzerland, 2010; pp 207–249.
- (3) Tanaka, H.; Takeichi, A.; Higuchi, K.; Motohiro, T.; Takata, M.; Hirota, N.; Nakajima, J.; Toyoda, T. *Sol. Energy Mater. Sol. Cells* **2009**, *93*, 1143–1148.

- (4) Tropsha, Y. G.; Harvey, N. G. *J. Phys. Chem. B* **1997**, *101*, 2259–2266.

- (5) The effects of dye desorption in limiting the practical utilization (i.e., commercialization) of DSCs have not been widely recognized since they are generally missed by light-flooding and other accelerated testing protocols. According to H. Desilvestro in ref 2, p 215, dye desorption due to moisture infiltration over extended periods of time leads to H<sub>2</sub>O accumulation inside cells, which, in turn, can result in dye desorption and unwanted chemical side reactions.

- (6) Law, C.; Pathirana, S. C.; Li, X.; Anderson, A. Y.; Barnes, P. R. F.; Listorti, A.; Ghaddar, T. H.; O'Regan, B. C. *Adv. Mater.* **2010**, *22*, 4505–4509.

- (7) Park, S.-H.; Lim, J.; Song, I. Y.; Atmakuri, N.; Song, S.; Kwon, Y. S.; Choi, J. M.; Park, T. *Adv. Energy Mater.* **2012**, *2*, 219–224.

- (8) Son, H.-J.; Wang, X.; Prasittichai, C.; Jeong, N. C.; Aaltonen, T.; Gordon, R. G.; Hupp, J. T. *J. Am. Chem. Soc.* **2012**, *134*, 9537–9540.

- (9) Liu, C.; Tsai, F.-Y.; Lee, M.-H.; Lee, C.-H.; Tien, T.-C.; Wang, L.-P.; Tsai, S.-Y. *J. Mater. Chem.* **2009**, *19*, 2999–3003.

- (10) Groner, M. D.; Fabreguette, F. H.; Elam, J. W.; George, S. M. *Chem. Mater.* **2004**, *16*, 639–645.

- (11) Ritala, M.; Leskelä, M. *Nanotechnology* **1999**, *10*, 19–24.

- (12) Niinistö, L.; Päiväsäari, J.; Niinistö, J.; Putkonen, M.; Nieminen, M. *Phys. Stat. Sol. (a)* **2004**, *201*, 1443–1452.

- (13) Jeong, N. C.; Son, H.-J.; Prasittichai, C.; Lee, C. Y.; Jensen, R. A.; Farha, O. K.; Hupp, J. T. *J. Am. Chem. Soc.* **2012**, *134*, 19820–19827.

- (14) While this paper was in review, a related study appeared, centering on inorganic dye desorption in water: Hanson, K.; Losego, M. D.; Kalayan, B.; Ashford, D. L.; Parsons, G. N.; Meyer, T. J. *Chem. Mater.* **2013**, *25*, 3–5.

- (15) Lyon, L. A.; Hupp, J. T. *J. Phys. Chem. B* **1999**, *103*, 4623–4628.

- (16) Lee, K.; Kim, J. Y.; Park, S. H.; Kim, S. H.; Cho, S.; Heeger, A. J. *Adv. Mater.* **2007**, *19*, 2445–2449.

- (17) Henrich, V. E.; Cox, P. A. *The Surface Science of Metal Oxides*; Cambridge University Press: Cambridge, UK, 1994.

- (18) Noguera, C. *Physics and Chemistry of Oxide Surfaces*; Cambridge University Press: Cambridge, UK, 1996.

- (19) Linsebigler, A. L.; Lu, G.; Yates, J. T., Jr. *Chem. Rev.* **1995**, *95*, 735–758.

- (20) Initially we employed trimethylaluminum (TMA) and water as metal-oxide precursors and attempted to grow Al<sub>2</sub>O<sub>3</sub> on TiO<sub>2</sub>:OrgD by ALD. We discovered that reactive adsorption of TMA diminishes absorption intensities, presumably by releasing methyl radicals that attack proximal dye molecules. While we found that the problem could be remedied by using a dimethylaluminum isopropoxide in place of TMA, we ultimately abandoned TMA because of the potential for dissolution of deposited alumina in strongly basic aqueous solutions.

- (21) Reichardt, C. *Chem. Rev.* **1994**, *94*, 2319–2358.

- (22) Pechy, P.; Rotzinger, F. P.; Nazeeruddin, M. K.; Kohle, O.; Zakeeruddin, S. M.; Humphry-Baker, R.; Grätzel, M. *Chem. Commun.* **1995**, 65–66.

- (23) Gillaizeau-Gauthier, I.; Odobel, F.; Alebbi, M.; Argazzi, R.; Costa, E.; Bignozzi, C. A.; Qu, P.; Meyer, G. J. *Inorg. Chem.* **2001**, *40*, 6073–6079.

- (24) Yan, S. G.; Prieskorn, J. S.; Kim, Y.; Hupp, J. T. *J. Phys. Chem. B* **2000**, *104*, 10871–10877.

- (25) Trammell, S. A.; Moss, J. A.; Yang, J. C.; Nakhle, B. M.; Slate, C. A.; Odobel, F.; Sykora, M.; Erickson, B. W.; Meyer, T. J. *Inorg. Chem.* **1999**, *38*, 3665–3669.

- (26) Heimer, T. A.; D'Arcangelis, S. T.; Farzad, F.; Stipkala, J. M.; Meyer, G. J. *Inorg. Chem.* **1996**, *35*, 5319–5324.

- (27) McNamara, W. R.; Snoberger, R. C., III; Li, G.; Schleicher, J. M.; Cady, C. W.; Poyatos, M.; Schmuttenmaer, C. A.; Crabtree, R. H.; Brudvig, G. W.; Batista, V. S. *J. Am. Chem. Soc.* **2008**, *130*, 14329–14338.

- (28) Sokolow, J. D.; Trzop, E.; Chen, Y.; Tang, J.; Allen, L. J.; Crabtree, R. H.; Benedict, J. B.; Coppens, P. *J. Am. Chem. Soc.* **2012**, *134*, 11695–11700.

- (29) McNamara, W. R.; Snoberger, R. C., III; Li, G.; Richter, C.; Allen, L. J.; Milot, R. L.; Schmuttenmaer, C. A.; Crabtree, R. H.; Brudvig, G. W.; Batista, V. S. *Energy Environ. Sci.* **2009**, *2*, 1173–1175.